Available online at www.sciencedirect.com
SCIENCE DIRECT®
Bioorganic & Medicinal Chemistry
ELSEVIER
Bioorganic & Medicinal Chemistry 12 (2004) 1337–1342

Engineering charge selectivity in model ion channels

Tyler Lougheed, Zhihua Zhang, G. Andrew Woolley* and Vitali Borisenko

Department of Chemistry, 80 St. George St. University of Toronto, Toronto, Ontario, Canada M5S 3H6

Received 26 February 2003; revised 3 June 2003; accepted 8 June 2003

Abstract—Most ion channel proteins exhibit some degree of charge selectivity, that is, an ability to conduct ions of one charge more efficiently than ions of the opposite charge. The structural origins of charge selectivity remain incompletely understood despite recent advances in the determination of cation-selective and anion-selective channel protein structures. Helix bundle channels formed via self-assembly of the peptide alamethicin provide a tractable model system for exploring the structural basis of charge selectivity. We synthesized covalently-linked alamethicin dimers, with amino acid substitutions at position 18 [lysine (Lys), arginine (Arg), glutamine (Gln), 2,3-diaminopropionic acid (Dpr)] in each helix, to assess the role of this position as a charge-selectivity determinant in alamethicin channels. Of the position 18 substitutions investigated, the Lys derivative exhibited the greatest degree of anion selectivity. Arg-containing channels were slightly less anion-selective than Lys. Interestingly, Dpr channels showed cation selectivity nearly equivalent to that exhibited by the neutral Gln derivative. We suggest that this result is due to a wider pore diameter that permits a greater number of counter-ions leading to enhanced charge screening and a lower effective side-chain positive charge.

1. Introduction

Ion channels comprise a unique class of protein structures, intrinsic to the cellular membranes of plants, animals and bacteria, which facilitate the passive transmembrane transport of ions down their electrochemical gradients. These molecular devices play roles in a host of diverse processes including nerve and muscle excitation, hormonal secretion, sensory transduction, and cell volume regulation.[1] The critical functional feature of ion channels is their ability to permit rapid transmembrane ion flux while remaining highly ion-selective.[2] Selectivity is determined by the interactions between ions, the channel and water- an inherently complicated physico-chemical system.[3] Detailed structural information has only recently become available for a few highly ion-selective channel proteins, including the bacterial potassium channel KcsA,[4–6] two members of the ClC chloride channel family[7] and most recently of a calcium-gated potassium channel MthK.[8] These studies represent a significant achievement in the field of structural biology, providing a detailed look at pore structures. However, the complexity of these structures, and the fact that mutations can affect regulation and gating in addition to permeation properties, can make systematic analysis of the structural origins of ion selectivity in these systems difficult.

We and others have elected to explore the origins of ion charge selectivity using smaller channel-forming peptides, either designed or natural, that can serve as model systems. The hope is that these minimal models will successfully recapitulate many of the crucial elements defining the pore structure of more complex biological channels, while superfluous features are eliminated or replaced with sequences of minimal complexity.[9] Over the past two decades, substantial effort has been extended towards understanding the biophysical properties of various channel-forming peptides,[3,9–11] In particular, these systems have been used to explore the role of electrostatics in determining charge selectivity.

Lear and DeGrado introduced a purely synthetic model system in which a suite of independently folded α-helical building blocks, in the form of a bundle of amphipathic helices, would generate a stable, hydrophilic transmembrane pore.[12] The peptide Ac-(Leu-Ser-Ser-Leu-Leu-

Keywords: Alamethicin; Ion-channel; Selectivity; Single-channel.
Abbreviations: Dpr, (L)-2; 3-diaminopropionic acid; Aib, α-aminoisobutyric acid; Alm, alamethicin; DMF, dimethylformamide; DCM, dichloromethane; DiPEA, diisopropylethylamine; ESI, electrospray ionization; Fmoc, 9-fluorenylmethyloxycarbonyl; HATU, *O*-(7-azabenzotriazol-1-yl)-*N*, *N*, *N*′, *N*′-tetramethyluronium hexafluorophosphate; HPLC, high performance liquid chromatography; *I*–*V*, current–voltage; MeOH, Methanol; TFA, trifluoroacetic acid.
* Corresponding author. Tel./fax: +1-416-978-0675; e-mail: awoolley@chem.utoronto.ca

0968-0896/$ - see front matter © 2003 Elsevier Ltd. All rights reserved.
doi:10.1016/j.bmc.2003.06.005

Ser-Leu)$_3$-CONH$_2$ was designed with a three-heptad repeat consisting of hydrophobic and neutral amino acids with the expectation that this would promote favorable inter-helix packing, along the entire helix length.[13] One predominant conductance state was observed when Ac-(Leu-Ser-Ser-Leu-Leu-Ser-Leu)$_3$-CONH$_2$ was added to planar lipid bilayers and this was proposed to be due to a parallel hexameric arrangement of peptides with a central pore 8 Å in diameter based on modeling, the observed voltage-dependence of peptide insertion into the membrane, and the measured permeability of ions of different sizes.[14,15]

Charge selectivity was calculated by recording single-channel *I–V* curves in asymmetric KCl solutions in order to measure reversal potentials.[14] The measured reversal potential gave a permeability ratio $P_{K}^{+}/P_{Cl}^{-} = 16$ using the Goldman–Hodgkin–Katz equation.[2] To further investigate permeation and selectivity of this model system, Lear and DeGrado prepared two different peptides, each bearing a formal charge at the N-terminus; Ac-Glu-Trp-(Leu-Ser-Ser-Leu-Leu-Ser-Leu)$_3$-CONH$_2$ and Ac-Arg-Trp-(Leu-Ser-Ser-Leu-Leu-Ser-Leu)$_3$-CONH$_2$.[16] It was postulated that addition of a positive charge should decrease cation selectivity and incorporating a negative charge would increase cation selectivity irrespective of which side the ion entered the channel. These predictions were borne out with Ac-Glu-Trp-(Leu-Ser-Ser-Leu-Leu-Ser-Leu)$_3$-CONH$_2$ showing strong cation selectivity and Ac-Arg-Trp-(Leu-Ser-Ser-Leu-Leu-Ser-Leu)$_3$-CONH$_2$ being non selective.

In an effort to introduce anion selectivity into a peptide model system, we explored the effects of side-chain mutations on the properties of channels formed by the peptide alamethicin. Alamethicin (Alm), originally isolated from the fungus *Trichoderma viride*, belongs to a family of channel-forming peptides referred to as peptaibols; peptides characterized by their high proportion of α-aminoisobutyric acid (*Aib*) residues and their C-terminal amino-alcohol cap. The generally accepted channel structure, like that of the Leu-Ser peptides, is a bundle of parallel helical alamethicin monomers commonly referred to as a barrel-stave structure.[3,11,17,18] We have previously detailed a covalent dimerization strategy that stabilizes channel structures composed of an even number of alamethicin peptides.[19] A model of an octameric bundle composed of four covalent dimers in shown in Figure 1.

We identified position 18 in the sequence as a position where mutations could alter charge selectivity. Native alamethicin has Gln in this position and is mildly cation selectivity with P_{K}^{+}/P_{Cl}^{-} of 4.3. Channels formed by Alm-K18, a mutant with lysine at position 18 in place of glutamine, were found to be anion selective with P_{Cl}^{-}/P_{K}^{+} of 3.7 at neutral pH.[20]

We now report further modifications at position 18 to provide a more systematic investigation into the role of this position as a selectivity determinant in alamethicin channels. We have constructed a series of alamethicin dimers, tethered via the same strategy and containing arginine, glutamine, lysine or 2,3 diaminopropionic acid (Dpr) at position 18. The results are discussed in relation to the previously published data on alm-K18 and we address the question as to whether a more anion selective channel of comparable complexity can be developed.

2. Results and discussion

2.1. Channel properties in symmetrical KCl solutions

We synthesized four alamethicin analogues with amino acid substitutions at position 18 using the same covalent dimerization strategy previously developed. The sequences of the peptides are shown in Figure 2.[19,21] Covalent linkage of alamethicin monomers extends the single-channel lifetime, which facilitates measuring single-channel *I–V* relationships. The linker used in the present study (Ac-Lys-Gly-Lys-COO$^-$) bears a formal negative charge whereas in the previous case with Alm-K18, the C-terminal linker functionality was a neutral amide (Ac-Lys-Gly-Lys-CONH$_2$). This change was made since higher yields were obtained with the chlorotrityl resin employed. To investigate what influence the charged linker might have, we compared the channel properties of Alm-K18 (neutral linker) with Alm-K18 (negative linker) in symmetrical 1 M KCl solutions. The pattern of channel formation with the negative linker is typical of dimeric alamethicin derivatives; even-number conducting bundles are selectively stabilized (data not shown). The current–voltage relationship of a putative hexamer level of the Alm-K18 (neutral) and Alm-K18 (negative) in 1 M KCl are compared in Figure 3. The curves are virtually superimposable, which implies that the electrostatic profile experienced by a mobile ion as it traverses the length of the channel is similar in each

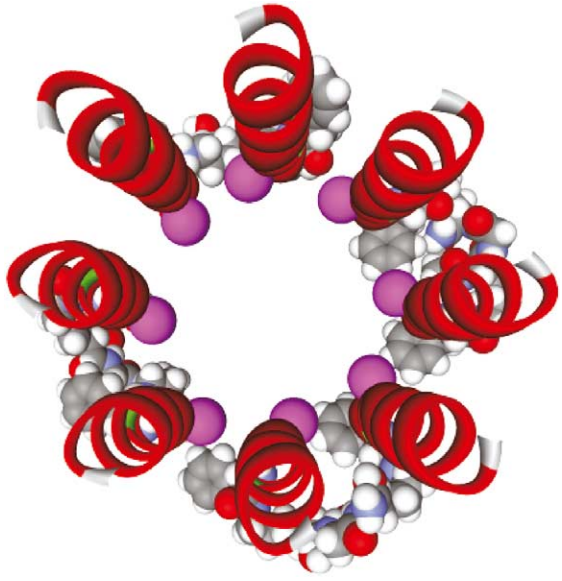

Figure 1. Model of the octameric (four dimers) conducting state of the alamethicin channel. The linkers are shown in space-fill and the peptide backbones are shown as ribbons. The position of residue 18 is indicated by a sphere located at the site of the β-carbon in each monomer. The view is from the N-terminal ends of the peptides.

A

Ac-Aib-Pro-Aib-Ala-Aib-Ala-Gln-Aib-Val-Aib-Gly-Leu-Aib-Pro-Val-Aib-Aib-Lys-Gln-Phe-C(O)NH-(CH_2)-CH(NHAc)-C(=O)-NH-CH_2-C(=O)-NH-CH(C(=O)NH_2)-(CH_2)-Ac-Aib-Pro-Aib-Ala-Aib-Ala-Gln-Aib-Val-Aib-Gly-Leu-Aib-Pro-Val-Aib-Aib-Lys-Gln-Phe-C(O)NH-(CH_2)-CH(NHAc)-C(=O)-NH-CH_2-C(=O)-NH-CH(C(=O)O^-)

B

Ac-Aib-Pro-Aib-Ala-Aib-Ala-Gln-Aib-Val-Aib-Gly-Leu-Aib-Pro-Val-Aib-Aib-Xxx-Gln-Phe-C(O)NH-(CH_2)-CH(NHAc)-C(=O)-NH-CH_2-C(=O)-NH-CH(C(=O)NH_2)-(CH_2)-Ac-Aib-Pro-Aib-Ala-Aib-Ala-Gln-Aib-Val-Aib-Gly-Leu-Aib-Pro-Val-Aib-Aib-Xxx-Gln-Phe-C(O)NH-(CH_2)-CH(NHAc)-C(=O)-NH-CH_2-C(=O)-NH-CH(C(=O)O^-)

Figure 2. Primary structures of covalently linked alamethicin peptides: (a) alm-K18 (neutral linker) (b) alm-X18 (negative linker). Xxx indicates the presence of lysine, arginine, glutamine or 2,3-diaminpropionic acid at position 18.

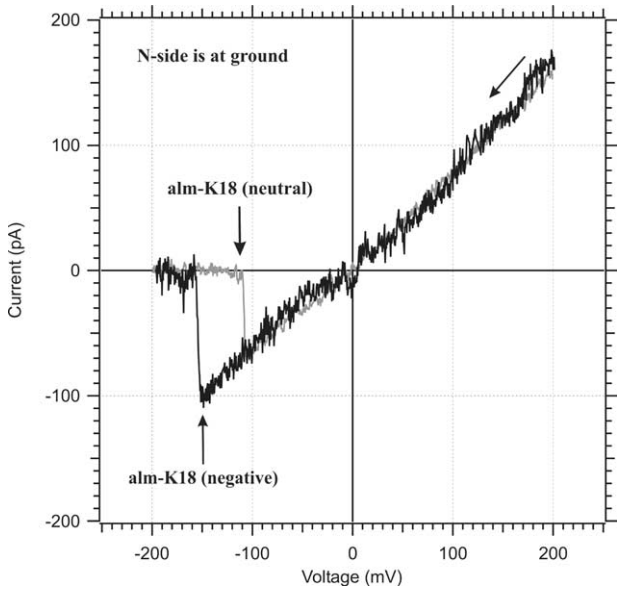

Figure 3. Representative single-channel *I–V* curves comparing the conduction properties of alm-K18 (negative linker) and alm-K18 (neutral linker) in symmetrical 1 M KCl solutions (5 mM BES at pH 7). The diagonal arrow indicates the direction of the voltage ramp.

case. As expected, the channels have fairly linear *I–V* curves resulting from a more symmetric electrostatic potential profile imposed by the Lys substitution[21] as compared to the native (Gln) channel. The similarity between these two channels is most easily explained as the result of charge screening of the negative linker by the bulk salt solution. This negative charge is expected to reside at the membrane surface and thus can be easily accessed by counter-ions. We have demonstrated previously that small changes in the linker structure have little effect on channel conductance properties,[22] which in light of these results can be extended to include linkers bearing formal negative charges.

2.2. Charge selectivity measured in a KCl gradient

We measured *I–V* relationships in KCl salt gradients using techniques described previously[20] to assess charge selectivity. Figure 4 shows *I–V* relationships measured at pH 7.0 for Alm-K18, Alm-R18, Alm-Q18, and Alm-Dpr18 in the presence of a 0.01–1.3 M KCl gradient. Reversal potentials are collected in Table 1 together with the calculated selectivity ratios. The particular alamethicin-conducting species for the gradient experiments has tentatively been assigned to a bundle of eight helices (Fig. 1), however a complete analysis of the conducting levels for each peptide is beyond the scope of this report. It should be noted, however, that selectivity has been shown to be rather insensitive to the molecularity of the conducting Alm species, at least in this size range.[20] Interestingly, while the charge on the linker has little effect on the conductance properties of the channel in symmetrical 1 M KCl solutions, charge selectivity measured in a gradient is influenced. The reversal potential measured previously for Alm-K18 (neutral) was −32 mV,[21] which indicates that Alm-K18 (negative) is less anion selective than its neutral analogue. As previously stated, this negative charge resides near the C-terminus, which in asymmetrical salt experiments is at the low salt side of the membrane. This reduced level of anion selectivity may thus be the result of less effective screening of the linker negative charge due to the lower ionic strength solution.

From this series of substitutions we see that Lys at position 18, irrespective of the charge on the linker, confers the highest degree of anion selectivity. Channels with Gln at position 18 are cation selective as expected. The degree of cation selectivity observed here is higher than that observed with Alm-Q18 linked by a neutral linker (alm-BAPHDA),[21] again indicating that the negative charge on the linker can enhance cation selectivity under conditions where screening of the linker is less effective.

The Alm-R18 mutant is also anion selective albeit less so than Alm-K18. While both amino acids are expected to be positively charged at pH 7, the positive charge on the Arg side chain is distributed among the three nitrogen atoms of the guanidinium group via resonance. This delocalization results in a lower charge density in comparison to the ammonium group of Lys that can lead to weaker electrostatic interactions.[23,24] In addition, the guanidinium group is the most highly solvated amino acid side chain in aqueous media due to extensive hydrogen bonding from the five potential hydrogen bond donors.[25] Perhaps the local concentration of arginine residues within the Alm-R18 channel pore causes a significant reorganization of water molecules that has either electrostatic implications or causes conformational changes within the channel structure.

Surprisingly, Alm-Dpr18 is nearly as cation selective as the native Alm-Q18. Side-chain amino groups are subject to the moderate inductive effects of both the α-NH_2 and CO_2^- functionalities. The pK_a of the β-amino group of free Dpr is 9.6 while that of the methyl ester is 8.25.[26] When incorporated into a peptide, one would expect the pK_a of the β-NH_2 to be raised slightly from that of the methyl ester derivative and thus, at pH 7.0, it would be expected to exist predominantly in its protonated form. Electrostatic interactions between multiple Dpr side chains in the channel might perturb the pK_as. Such effects were analyzed previously in the case of Alm-K18 (with a neutral linker).[20] At high pH, where Lys is uncharged, the Alm-K18 channel exhibits wild-type (cation) selectivity whereas at pH values of 7 and below, channels display anion selectivity. Since no change in selectivity occurs between pH 7 and 3, and since protons are expected to be in equilibrium with the open state of the channel during selectivity measurements, the channel is believed to be fully protonated (+8 charge for an octamer bundle) at pH 7. A similar behaviour is expected for Alm-Dpr18 channels.

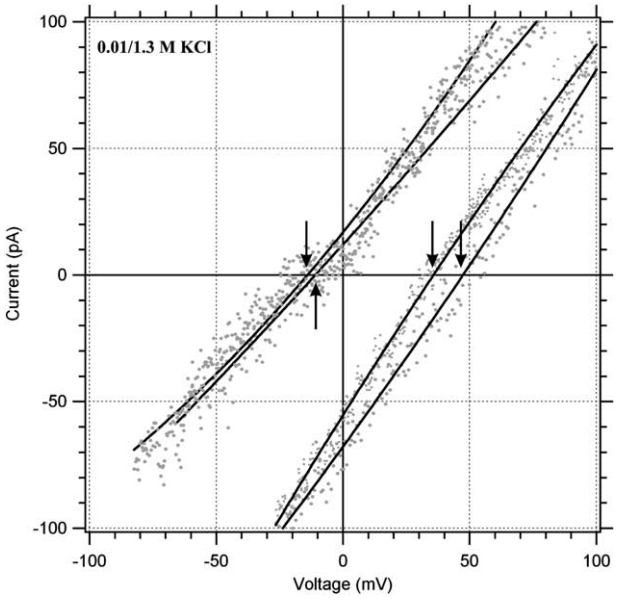

Figure 4. Single-channels *I–V* curves for the putative octamer level of alm-X18 (negative linker). Channels opened at 200 mV, whereupon the voltage was ramped to −200 mV (the direction of the voltage ramp is the same as for Fig. 3) over 30–80 ms and the current recorded. Channels generally close before −200 mV is reached and closing transitions have been deleted for clarity. The KCl concentration was 1.3 M at ground and 0.01 M on the opposite side, each buffered at 7.0 with 5 mM BES. Channels are oriented with N-terminal at ground and vertical arrows indicate reversal potentials. From left to right: alm-K18, alm-R18, alm-Dpr18, alm-Q18.

Recent molecular dynamics simulation studies by Tieleman et al. have shown that fully charged Alm-K18 channels appear to be stable in membranes and that significant counter-ion binding to Lys residues occurs depending on the charge state of the channel and the salt concentration.[27] Particularly, with 1 M KCl, the effective charge can be reduced by 4e$^-$ due to the presence of 4 Cl^- ions near the eight charged Lys residues.[27] Experimentally, anion selectivity is observed to decrease as ionic strength increases consistent with a charge-screening effect of the counter-ions on the field created by the lysine residues.[27] Since the Dpr side chain is shorter than Lys, a wider local pore diameter at position 18 is expected (Fig. 1). We propose that this wider lumen could accommodate an increased number of chloride ions to provide added screening of the positive charge and further reduce the level of anion selectivity. Of course, one cannot rule out that other factors may contribute to the experimentally observed selectivity. For instance, local conformational changes of the Lys side chains may be important and less pronounced in the case of Dpr as a result of the reduced side-chain length. Molecular models have shown that under certain conditions, Lys residues could reside at the center of the channel pore, which is likely inaccessible space to the shorter Dpr side chain.

With these results in hand, we can address the idea of how to construct a channel of comparable complexity to those described, yet achieve increased anion selectivity. The region of the channel near position 18 may be too spacious and allow for extensive charge shielding. All our molecular models of alamethicin channels, including those of Alm-K18, point towards a constriction near the Gln 7 side chain (Fig. 1). In fact, this area constitutes that narrowest part of the alamethicin channel. Recent work by Asami et al. has investigated alamethicin

Table 1. Selectivity properties of channels formed by Alm derivatives[b,c]

	Alm-Q18	Alm-Q18nl[a]	Alm-K18	Alm-K18nl[a]	Alm-R18	Alm-Dpr18
V_{rev} (mV)	+50	+35	−15	−32	−8	+30
P_{K^+}/P_{Cl^-}	8.1	4.3	0.54	0.27	0.72	3.5

[a] Linked with the neutral linker (all others linked with the negatively charged linker) (data from ref. 21).
[b] Measured in a 1.3 M/0.01 M KCl gradient as described in the Experimental.
[c] Calculated using the GHK equation as described.[21]

channels bearing a substitution of Glu 7 for Gln 7.[28] Selectivity of these channels was assessed by the current-ratio method using the bulky organic counter-ions potassium gluconate and *N*-methylglucosammonium chloride. Channels bearing a glutamate at position seven were found to have current ratios (I_{Kgluc}/I_{NmgCl}) of 4–5 indicative of channels that were cation selective. This selectivity decreased as the conductance-level number increased in line with the explanation of a wider pore radius. Incorporation of a significant amount of positive charge at this narrow part of K18 may furnish a more highly anion selective channel. Another approach may be to introduce a modification that constricts that channel to limit counter-ion binding.

3. Conclusions

Alamethicin channels constitute a useful model system to investigate the origins of charge selectivity. Covalent dimerization permits selective stabilization of conducting species and extends single-channel lifetimes into a range that facilitates the measurement of single-channel current–voltage relationships. Substitution of a neutral linker by[21] one bearing a negative charge, while having little effect on the electrostatic potential profile of alamethicin channels in symmetric 1 M salt solutions, results in reduced charge selectivity in KCl gradients. Lys at position 18 yields the greatest degree of anion selectivity. Arginine substitution generates channels slightly less anion selective, which is likely the result of specific interactions inherent to the guanidinium side chain. Substitution with Dpr results in a reversal of ion selectivity. The observed reversal of charge selectivity may be due to chloride ions compensating for the local charge density imposed by the side-chain amino groups in a relatively wide region of the channel pore. In order to create a highly anion selective channel it seems that it would be beneficial to impose a region of positive charge in a narrow part of the channel or to reduce counter-ion binding. Concomitantly it might be necessary to develop a more complex architecture that more closely resembles the selectivity filters of highly selective biological channels.

4. Experimental

4.1. Peptide synthesis

Alamethicin dimers were synthesized in a similar manner to that described in Starostin et al.[21] Briefly, the Ac-Lys-Gly-Lys-COO^- linker was assembled on the solid support followed by simultaneous, step-wise assembly of the two alamethicin monomers; each monomer extending from the ε-amino groups of the lysine side chains. The template was synthesized using a 2-chlorotrityl-chloride resin on a model ACT 90 peptide synthesizer (Advanced ChemTech). Fmoc-Lys-Dde (53 mg, 0.1 mmol, 0.6 equiv to resin) was dissolved in 1.3 mL dry DCM and added to 128 mg of resin with 70 μL of DiPEA. After 25 min of vigorous stirring, the resin was washed three times with DCM/MeOH/DiPEA (17:2:1), three times with DCM, two times with DMF and finally two times with MeOH (1.5 mL volume for each wash). The residual methanol was removed under high vacuum and the resin dried over KOH. The substitution of the resin was assessed by weight increase. Fmoc-Lys(Dde)-resin (0.05 mmol) was deprotected through addition of 10 mL of 5% piperidine in DCM/DMF (1:1) with stirring for 20 min, followed by 8.0 mL of 20% piperidine in DMF for 80 min. The remaining Gly and Lys residues of the linker were coupled using three equivalents of amino acid, three equivalents of HATU and six equivalents of DiPEA with Fmoc deprotection after each step as already described. The N-terminus was acetylated using an acetic anhydride/DiPEA/DMF (1:2:7) mixture for 30 min. Dde was the group used for orthogonal protection of the lysine side-chain functionality during template assembly. Deprotection was accomplished using a 2% hydrazine/DMF solution (2×10 min). The alamethicin chains were then assembled using five equivalents of the isolated Fmoc amino acid fluorides,[29] five equivalents of HATU and 10 equivalents of DiPEA at a concentration of 0.3 M (amino acid) in DMF. In the case of Aib residues, seven equivalents of the isolated amino acid were used. After the last coupling step, the N-termini were acetylated using the aforementioned procedure. Peptide cleavage from the resin was preformed by vigorous mixing in a 2% triisopropylsilane, 5% water in a 50% TFA, 50% DCM solution for 50 min. The crude peptide product was isolated by cold ether precipitation. Crude peptide mixtures were purified by HPLC with a Polyencap A300 column (4.6×125 mm) using a linear gradient (50–80%A in 30 min) in which eluent A consisted of 0.1% TFA in water while eluent B consisted of 80% acetonitrile/20% water containing 0.1% TFA. Each peptide registered a unique retention time: Alm-R18 = 16.5 min, Alm-Q18 = 16 min, Alm-K18 = 19 min, Alm-Dpr = 17 min. Prior to use in single-channel measurements, peptides were rechromatographed under the same conditions. ESI-MS data: Alm-R18 = $C_{202}H_{335}N_{55}O_{51}$ observed = 4349.1, calculated = 4350.16; Alm-Q18 = $C_{200}H_{325}N_{51}O_{53}$ observed = 4291.0, calculated = 4292.03; Alm-K18 = $C_{202}H_{333}N_{51}O_{51}$ observed = 4291.7, calculated = 4292.12; Alm-Dpr = $C_{196}H_{321}N_{51}O_{51}$ observed = 4207, calculated = 4207.96.

4.2. Single-channel measurements

Peptides (~0.1 μM in MeOH) were added to the ground-side of membranes formed from diphytanoyl phosphatidylcholine/decane (50 mg/mL). Polystyrene bilayer chambers with 150-μm apertures (Warner Instrument Co.) were used. Voltage was set using an Axopatch ID patch-clamp amplifier (Axon Instruments) controlled by Synapse software (Synergistic Research Systems) and currents were measured. A CV-4B-0.1/100 switchable headstage was used with the gain set to 0.1. All data was filtered at 1 kHz, sampled at 5× the filter frequency, stored directly to disk and analyzed using Synapse and Igor (Wavemetrics, Inc) software. All measurements were preformed at 22° C (±2 °C). Salt solutions were connected via agarose/KCl salt bridges to 1 M KCl salt reservoirs containing silver/silver chloride

electrodes. All salt solutions (0.01 and 1.3 M) contained 5 mM BES, pH = 7.0.

Single-channel current–voltage (*I–V*) curves were obtained using the following voltage-clamp protocol: a step from 0 to +200 mV, holding at 200 mV for 100–700 mS, then a ramp down to −200 mV over the course of 30–80 ms, followed by a return to 0 mV for several seconds. Capacitive currents obtained when no channels were open were subtracted from currents obtained with a single channel open during the ramp. With ramp times greater than 20 ms and the amplifier settings described above, the capacitive transient did not lead to amplifier saturation. This protocol measured the *I–V* relationship for channels oriented with their N-terminus at the high-salt side of the membrane. The N-terminus inserts through the membrane made positive by the applied field and the high-salt side (1.3 M KCl) is always at electrical ground.

References and notes

1. Ashcroft, F. M. *Ion Channels and Disease*; Academic: San Diego, CA, 2000.
2. Hille, B. *Ion Channels of Excitable Membranes*, 3rd ed.; Sinauer Associates, Inc: Sunderland, MA, 2001.
3. Sansom, M. S. P. *Quart. Rev. Biophys.* **1993**, *26*, 365.
4. Doyle, D. A.; Cabral, J. M.; Pfuetzner, R. A.; Kuo, A.; Gulbis, J. M.; Cohen, S. L.; Chait, B. T.; MacKinnon, R. *Science* **1998**, *280*, 69.
5. Zhou, Y.; Morais-Cabral, J. H.; Kaufman, A.; MacKinnon, R. *Nature* **2001**, *414*, 43.
6. Morais-Cabral, J. H.; Zhou, Y.; MacKinnon, R. *Nature* **2001**, *414*, 37.
7. Dutzler, R.; Campbell, E. B.; Cadene, M.; Chait, B. T.; MacKinnon, R. *Nature* **2002**, *415*, 287.
8. Jiang, Y.; Lee, A.; Chen, J.; Cadene, M.; Chait, B. T.; MacKinnon, R. *Nature* **2002**, *417*, 515.
9. Akerfeldt, K. S.; Lear, J. D.; Wasserman, Z. R.; Chung, L. A.; DeGrado, W. F. *Acc. Chem. Res.* **1993**, *26*, 191.
10. Montal, M. *Curr. Opin. Struct. Biol.* **1995**, *5*, 501.
11. Woolley, G. A.; Wallace, B. A. *J. Membrane Biol.* **1992**, *129*, 109.
12. Lear, J. D.; Wasserman, Z. R.; DeGrado, W. F. *Science* **1988**, *240*, 1177.
13. Cohen, C.; Parry, D. A. D. *Trends Biochem. Sci.* **1986**, *11*, 245.
14. Kienker, P. K.; Lear, J. D. *Biophys. J.* **1995**, *68*, 1347.
15. Akerfeldt, K. S.; Kienker, P. K.; Lear, J. D.; DeGrado, W. F. *Comprehensive Supramolecular Chemistry*; Pergamon: London, 1996.
16. Lear, J. D.; Schneider, J. P.; Kienker, P. K.; DeGrado, W. F. *J. Am. Chem. Soc.* **1997**, *119*, 3212.
17. Latorre, R.; Alvarez, O. *Physiol. Rev.* **1981**, *61*, 77.
18. Sansom, M. S. P. *Prog. Biophys. Mol. Biol.* **1991**, *55*, 139.
19. You, S.; Peng, S.; Lien, L.; Breed, L.; Sansom, M. S. P.; Woolley, G. A. *Biochemistry* **1996**, *35*, 6225.
20. Borisenko, V.; Sansom, M. S. P.; Woolley, G. A. *Biophys. J.* **2000**, *78*, 1335.
21. Starostin, A. V.; Butan, R.; Borisenko, V.; James, D. A.; Wenschuh, H.; Sansom, M. S. P.; Woolley, G. A. *Biochemistry* **1999**, *38*, 6144.
22. Jaikaran, D. C. J.; Biggin, P. C.; Wenschuh, H.; Sansom, M. S. P.; Woolley, G. A. *Biochemistry* **1997**, *36*, 13873.
23. Schmidtchen, F. P.; Berger, M. *Chem. Rev.* **1997**, *97*, 1609.
24. Dietrich, B.; Fyles, D. L.; Fyles, T. M.; Lehn, J.-M. *Helv. Chim. Acta* **1979**, *62*, 2763.
25. Hannon, C. L.; Anslyn, E. V. *Bioorganic Chemistry Frontiers* **1993**, *3*, 193.
26. Hay, R. W.; Morris, P. J. *J.C.S. Perkin II* **1972**, *8*, 1021.
27. Tieleman, D. P.; Borisenko, V.; Sansom, M. S. P.; Woolley, G. A. *Biophys. J.* **2003**, *84*, 1464.
28. Asami, K.; Okazaki, T.; Nagai, Y.; Nagaoka, Y. *Biophys. J.* **2002**, *83*, 219.
29. Wenschuh, H.; Beyermann, M.; Krause, E.; Brudel, M.; Winter, R.; Schumann, M.; Carpino, L. A.; Bienert, M. *J. Org. Chem.* **1994**, *59*, 3257.